JPP Journal of Pharmacy and Pharmacology

Journal of Pharmacy and Pharmacology, 2021, Vol XX, 1–9
https://doi.org/10.1093/jpp/rgab121
Research Paper
Advance Access publication 1 September 2021

OXFORD

Research Paper

Semi-solid extrusion 3D printing of starch-based soft dosage forms for the treatment of paediatric latent tuberculosis infection

Aikaterini-Theodora Chatzitaki[1], Emmanouela Mystiridou[2], Nikolaos Bouropoulos[2,3], Christos Ritzoulis[4], Christina Karavasili[1,*] and Dimitrios G. Fatouros[1]

[1]Laboratory of Pharmaceutical Technology, Department of Pharmacy, School of Health Sciences, Aristotle University of Thessaloniki, Thessaloniki, Greece
[2]Department of Materials Science, University of Patras, Patras, Greece
[3]Foundation for Research and Technology Hellas, Institute of Chemical Engineering and High Temperature Chemical Processes, Patras, Greece
[4]Department of Food Science and Technology, International Hellenic University, Thessaloniki, Greece

*Correspondence: C. Karavasili, Laboratory of Pharmaceutical Technology, Department of Pharmacy, School of Health Sciences, Aristotle University of Thessaloniki, Thessaloniki GR-54124, Greece. Tel: +30-2310-990362; Email: karavasc@pharm.auth.gr

Received April 26, 2021; Accepted July 29, 2021.

Abstract

Objectives The development of age-appropriate dosage forms is essential for effective pharmacotherapy, especially when long-term drug treatment is required, as in the case of latent tuberculosis infection treatment with up to 9 months of daily isoniazid (ISO). Herein, we describe the fabrication of starch-based soft dosage forms of ISO using semi-solid extrusion (SSE) 3D printing.

Methods Corn starch was used for ink preparation using ISO as model drug. The inks were characterized physicochemically and their viscoelastic properties were assessed with rheological analysis. The morphology of the printed dosage forms was visualized with scanning electron microscopy and their textural properties were evaluated using texture analysis. Dose accuracy was verified before in-vitro swelling and dissolution studies in simulated gastric fluid (SGF).

Key findings Starch inks were printed with good resolution and high drug dose accuracy. The printed dosage forms had a soft texture to ease administration in paediatric patients and a highly porous microstructure facilitating water penetration and ISO diffusion in SGF, resulting in almost total drug release within 45 min.

Conclusions The ease of preparation and fabrication combined with the cost-effectiveness of the starting materials constitutes SSE 3D printing of starch-based soft dosage forms a viable approach for paediatric-friendly formulations in low-resource settings.

Keywords: semi-solid extrusion 3D printing; soft tablets; tuberculosis; paediatric drug delivery; patient compliance

Introduction

Additive manufacturing technologies (AMT) have opened up new avenues in shaping the way health care could be delivered. The introduction of innovative practices to address challenges commonly encountered in healthcare provision offers the potential to improve the coverage, quality, accessibility and affordability of the medical services provided especially in at-risk patient populations, such as the paediatric and geriatric, and low-resource settings. Personalization of drug treatment in terms of dosage strength, dimensions, organoleptic properties and ease of administration has to be the major asset that AMT contribute to healthcare improvement, compared with the stringent procedures followed in conventional pharmaceutical manufacturing.[1] At the same time, problems related to distance and access may be resolved by providing the opportunity for decentralized drug manufacturing in point-of-care settings, such as a hospital pharmacy. Equally important to overcoming geographical barriers in healthcare access is to assure the financial accessibility of the drug products and services to those in need of them, without any compromise in their quality.

Semi-solid extrusion (SSE) 3D printing conglomerates all the aforementioned assets in a single technique. The semi-solid nature of the feedstock material enables printing at low temperatures within a few minutes without compromising printing accuracy.[2–4] SSE 3D printing has been employed for the fabrication of polypills with defined drug release[5, 6] and tablets with immediate drug release profiles,[7, 8] enabling layer-wise dose adjustments with high precision.[9] Even though still in its infancy in the pharmaceutical field, it was recently that the first clinical study using SSE 3D printing was conducted in children with a rare metabolic disease within a hospital setting. Children were administered with the 3D printed chewable dosage forms, showing specific preferences over certain colour and flavour profiles, while the therapeutic efficacy of the printlets was similar to conventional capsules prepared by manual compounding, yet showing less variability.[10] Ease of administration is a critical factor affecting patient compliance and therefore clinical efficacy, especially among paediatric patients.[11] This was clearly exemplified in a visual preferences study of 3D printed tablets prepared using digital light processing (DLP), selective laser sintering, SSE and fused deposition modelling (FDM) that was conducted among 368 children aged 4 to 11 years old. DLP printlets got the highest preference (61.7%) among children, whereas FDM printlets the lowest (5.4%). However, most of the participants changed their selection over SSE printlets once they were informed that the latter were chewable and therefore easier to ingest, further confirming children's inclination towards chewable dosage forms.[12] Within this context, an SSE 3D printed chewable drug delivery platform was fabricated based on chocolate, aiming to provide a paediatric-friendly oral dosage form that would appeal to children's preferences in terms of appearance and taste.[13]

An ideal paediatric formulation should consist of non-toxic excipients, enable ease of administration and flexible and accurate dose titration over a wide age and weight range, while at the same time its production should be easy, cost-effective and commercially viable.[14] This study aims to address these requirements from both a material and manufacturing method perspective, describing the fabrication of starch-based soft dosage forms for paediatric tuberculosis treatment with isoniazid (ISO) using SSE 3D printing. 3D printed dosage forms for the administration of ISO[15] or the co-administration of ISO and rifampicin[16, 17] have been previously fabricated with hot melt extrusion coupled with FDM 3D printing. However, in all cases, the 3D printed dosage forms would have to be swallowed intact, which is one of the primary reasons for medicine rejection among paediatric patients commonly encountering swallowing difficulties for solid dosage forms.[11] In this study, corn starch was used as a low-cost pharmaceutical excipient, commonly employed as binder and disintegrant and generally recognized as safe ingredient.[18] Its ability to form extrudable hydrogels upon heating was exploited for the fabrication of 3D printed soft dosage forms that would be easy to administer in paediatric patients with high dose accuracy. This is of high importance especially among children with latent tuberculosis infection undergoing long-term therapy of up to 9 months of daily ISO for whom compliance to the therapeutic scheme is intertwined with a successful therapeutic outcome.[19] The ease of preparation and fabrication combined with the cost-effectiveness of the starting materials proposed in this study constitutes SSE 3D printing of personalized dosage forms a viable alternative to manual compounding in hospital settings and an applicable solution in low-resource settings.

Materials and Methods

Materials

ISO was obtained from Fagron HELLAS (Athens, Greece). Corn starch was kindly gifted by Rontis Hellas SA (Larisa, Greece). All other reagents were of analytical grade and distilled water was used in all studies.

Characterization of starch

Particle size distribution

Starch (20 g) was placed on the uppermost sieve of a sieve stack with decreasing apertures (0.212–0.025 mm) and shaken for 1 min in a sieve shaker (FRITSCH GmbH, Germany). Sample mass retained on each sieve was quantified and the particle size distribution was calculated.

Preparation of the blank and ISO starch inks

Starch was mixed with distilled water (1:4 w/w)[20] and the dispersions were then kept under magnetic stirring in a water bath at 86 ± 1°C for 20 min to ensure complete gelatinization.[21] The obtained ink was cooled down at RT before cartridge filling. The ISO starch ink was prepared following the exact same procedure by first dissolving ISO (100 mg/mL) in water. The amount of water loss during ink preparation was calculated gravimetrically at the end of the preparation process.

Pressure-assisted microsyringe 3D printing

Starch tablets were fabricated using the CELLINK INKREDIBLE printer (Gothenburg, Sweden). Stereolithography templates were obtained from an open-source database (https://www.thingiverse.com/) and imported into Cellink HeartWare software for slicing. Starch inks were extruded from 3 mL cartridges through a 25G nozzle at a pressure of 102 kPa. The layer height was set at 0.4 mm, and the infill pattern and content were adjusted to concentric and 100%, respectively. The printing speed was set at 6 mm/s, and the printing rate was calculated to be 0.066 ± 0.004 gr/min from the ratio of the printed mass to the printing time (n = 4). Tablet dimensions were determined by measuring three individual tablets with a digital micrometer.

Scanning electron microscopy

The printed tablets were freeze-dried and visualized by means of scanning electron microscope (SEM; field emission SEM, LEO 1530VP). The accelerating voltage was set at 15 kV. Samples were mounted on metallic sample stands using carbon conductive tabs (PELCO Image Tabs) and gold sputtered under high vacuum (~$5{\cdot}10^{-2}$ mbar) using a BAL-TECSCD-004 sputtering unit.

Physicochemical characterizations

Fourier transform infrared spectroscopy

Fourier transform infrared spectroscopy (FTIR) spectroscopy was performed using a Shimadzu IR-Prestige-21 FTIR spectrometer (Shimadzu Europa GmbH, Duisburg, Germany) with a horizontal Golden-Gate MKII single reflection ATR system (Specac, Kent, UK) equipped with ZnSe lenses. The spectra were recorded in the range between 800 and 4000 cm^{-1} with a resolution of 4 cm^{-1} after 64 scans.

Differential scanning calorimetry

Differential scanning calorimetry (DSC) analysis was performed on a DSC 204 F1 Phoenix apparatus (NETZSCH, Germany). Samples were loaded on aluminium pans with perforated lids and were heated from 40°C to 200°C at a heating rate of 10°C/min under a nitrogen flow of 70 mL/min using an empty pan as a reference.

Thermogravimetric analysis

Thermogravimetric analysis (TGA) was conducted on a TGA Q500 (TA Instruments Ltd.) apparatus in the temperature range between 15°C and 800°C and at a heating rate of 10°C/min in air atmosphere.

X-ray diffraction analysis

X-ray diffraction (XRD) analysis was performed on the freeze-dried starch ink and dispersion samples using a D8-Advance instrument (Bruker, Germany) with Ni-filtered $CuKa_1$ radiation, operating at 40 kV and 40 mA. The diffraction spectra were recorded from 5° to 60°, at a step size of 0.02° and at a scanning speed of 0.35 s/step.

Texture profile analysis

Texture profile analysis (TPA) of the blank and ISO printed tablets (height: 6.4 mm and diameter: 11 mm) was performed using a TA.Xtplus Texture Analyzer (Stable Micro Systems, Godalming, UK) with a cylindrical probe (50 mm). Samples were compressed twice at a speed of 1 mm/s and deformation level was set at 40% of the initial tablet height. The TPA parameters (hardness: the first force peak height, cohesiveness: the ratio of the area of the first peak over the area of the second peak, springiness: the time value of the detected height during the second compression to the respective value during the first compression, gumminess: hardness × cohesiveness and adhesiveness: the negative area between two compressions) were calculated from the respective TPA curves.

Oscillation rheology

Small oscillatory viscoelastic flow was measured using a Bohlin CVOR 150 controlled strain rheometer (Malvern Ltd, Worcestershire, UK) equipped with a 4-cm diameter steel cone-and-plate geometry (4°), thermostated at 25°C. An initial strain amplitude sweep was performed to determine the linear viscoelastic region. Frequency sweeps were then carried out at strain value of 0.1% in the shear-independent plateau at a frequency range of 1 to 150 Hz.

Determination of drug content and dose accuracy

Precisely weighted amounts of the ISO printed tablets were mixed with 50 mL distilled water, vortexed till completely dispersed and centrifuged at 2000 *g* for 15 min. ISO content was quantified in the supernatants with UV spectrophotometry at 262 nm. ISO calibration curve in water was linear (R^2 = 0.9998) in the concentration range of 1–25 µg/mL. The same procedure was followed for the blank printed tablets to assure that there was no interference from the excipient. Drug content was further confirmed with TGA by measuring the difference in mass loss between the starch ink and ISO starch ink in the temperature range of 150–300°C, corresponding to the onset of ISO mass loss at 150°C, which reached a constant value after 300°C. Dose accuracy in the printed dosage forms was assessed according to a previously reported method.[9] Tablets were printed having the same diameter (11 mm) and increasing number of layers ranging from 1 to 16. ISO content (mg) was quantified following the same process as described above and results were plotted against the number of layers. Linear regression was used to predict the relationship between the two variables.

Water absorption capacity

The water absorption behaviour of the blank printed tablets was evaluated in simulated gastric fluid (SGF) pH 1.2 [2 g/L NaCl and 2.917 g/L HCl (37% w/w)] at 37°C. At pre-determined time intervals, tablets were collected and weighed after carefully blotting them dry to remove excess medium. Water absorption (%) was calculated by the percentage equivalent of the ratio of water weight gain to the initial weight of the tablet.

In-vitro dissolution studies

Dissolution studies were performed in SGF pH 1.2 (200 mL) at 37 ± 0.2°C using the USP II dissolution apparatus at a paddle rotational speed of 50 rpm. To simulate the mastication process, the ISO printed tablets were minced before the addition of the dissolution medium. Samples (2 mL) were withdrawn and replaced with equal volume of medium and then centrifuged at 2000 *g* for 15 min. ISO quantification in the supernatants was performed using UV spectrophotometry at 262 nm. ISO calibration curve in SGF was linear (R^2 = 0.9999) at the concentration range 5–25 µg/mL.

Statistical analysis

The data are presented as mean values ± S.D of at least three independent measurements. One-way ANOVA was performed to evaluate statistical significance at $P \leq 0.05$.

Results

Ink preparation and 3D printing process

The mean particle size of corn starch used for the preparation of the ink was calculated to be 75 µm. The starch ink was prepared at a 1:4 corn starch to water weight ratio under hydrothermal treatment. The starch inks showed good extrudability supporting the 3D printing of multi-layered self-standing constructs in the form of tablets (Figure 1C) or in more child-friendly designs (Figure 1B). The starch tablets used in all following studies were designed in a cylindrical shape with 16 layers (11 mm diameter × 6.4 mm height) and 0.72 ± 0.07 g weight, and the dimensions of the 3D printed objects were determined to be 11.3 mm ± 0.6 mm × 6.5 mm ± 0.2 mm using a digital calibre, corresponding to less than 5% deviation from the preset values.

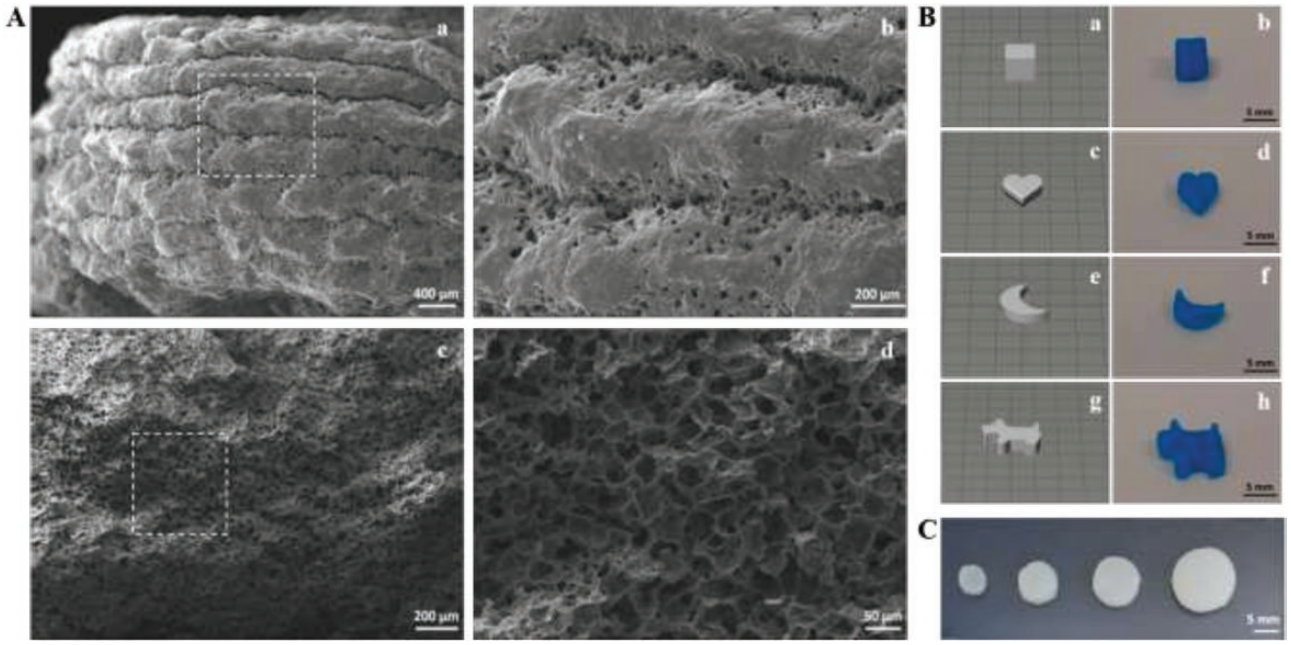

Figure 1 (A) Scanning electron microscopy images of the (a, b) external and (c, d) internal morphology of the 3D printed starch tablets, showing the distinctive deposition of the individual layers on the top of one another and their highly microporous internal structure. The dotted rectangles correspond to the higher magnification images on the right. (B) Schematic representation of (a, c, e and g) the .stl files and (b, d, f and h) the respective 3D printed dosage forms in the shape of (a, b) cube, (c, d) heart, (e, f) moon and (g, h) dog. A blue food colouring was used for contrast reasons. (C) The starch-based tablets printed in different sizes.

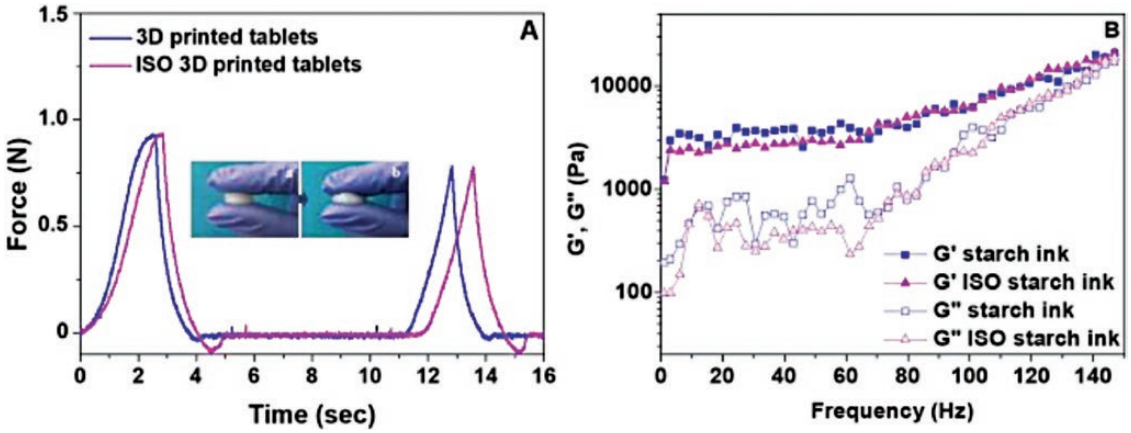

Figure 2 (A) TPA of the blank and ISO 3D printed starch tablets ($n = 3 \pm$ S.D.). The inset shows (a) the handling of the 3D printed starch tablets even (b) after the application of slight pressure. (B) Oscillation frequency sweep tests of the blank and ISO starch inks at a strain value of 0.1% and at the frequency range of 1 to 150 Hz (25°C).

SEM visualization

The 3D printed tablets were freeze-dried before SEM visualization of their surface [Figure 1A(a and b)] and internal morphology [Figure 1A(c and d)]. The tablets retained their structural integrity post-printing, as evident from the individual ink layers distinctively deposited on top of one another. Cross-section of the tablets revealed a highly porous internal microstructure with interconnected pores with diameters less than 45 µm.

Texture profile analysis

TPA was performed on the blank and ISO printed tablets (Figure 2A) to simulate the mastication process, and the textural parameters (hardness, cohesiveness, springiness, gumminess and adhesiveness) were calculated and presented in Table 1. As is evident from the values of the TPA parameters, ISO had no effect on the textural properties of the starch printed tablets. On the one hand, hardness is indicative of the maximum force that occurs during the first bite and specifically for starch gels is attributed to the swelling capacity of the starch granules,[22] whereas cohesiveness, on the other hand, relates to the gel's ability to withstand deformation during mastication. Both parameters were found to be significantly lower compared with the respective values of semi-solid foods well accepted by children, such as peanut butter (hardness: 3.46 ± 0.32 N, cohesiveness: 0.89 ± 0.04) and boiled mashed potato (hardness: 2.83 ± 0.09 N, cohesiveness: 0.76 ± 0.03).[23] Springiness relates to the elasticity of semi-solids, whereas gumminess and adhesiveness are representative

of the energy required for their disintegration and to break their attraction with the structures in the mouth (palate, tongue and teeth), respectively.[23] The adhesiveness of the printed tablets was found to be relatively lower to that of mango pudding (0.10 ± 0.10 mJ),[23] whereas their springiness and gumminess values were found to be similar and significantly lower, respectively, to those of a banana.[24]

Rheological analysis

The viscoelastic properties of the starch inks in the absence and presence of ISO were evaluated with oscillation amplitude frequency sweep testing (Figure 2B). Both samples exhibited similar rheological behaviour. All moduli increased with frequency, which is well expected of shear-thickening materials such as starch pastes.[25, 26] The starch ink showed slightly higher moduli up to 80 Hz, compared with ISO starch ink, but it should be noted that this difference was close to the margin of the device's accuracy. The samples were predominantly solid throughout the tested frequency range, as all elastic (G′) and viscous (G″) moduli are separated by at least one order of magnitude, up to about 100 Hz. From that frequency upwards, they match in order of size, forming a true gel (G′ ~ G″) at 150 Hz. This suggests that the relaxation times of the starch polymers in the matrix are close to 1/150 s ~ 7 ms in both cases, so any faster deformations will not be followed by a corresponding rearrangement of the macromolecules in their network, resulting in polymer flow.

Table 1 TPA parameters of the blank and ISO 3D printed tablets

TPA parameters	Formulation	
	Blank 3D printed tablets	ISO 3D printed tablets
Hardness (N)	0.94 ± 0.00	0.87 ± 0.11
Cohesiveness (–)	0.53 ± 0.05	0.57 ± 0.00
Springiness (s)	0.63 ± 0.02	0.70 ± 0.12
Gumminess (N)	0.50 ± 0.05	0.50 ± 0.06
Adhesiveness (N·s)	0.03 ± 0.03	0.04 ± 0.01

n = 3 ± S.D.

Physicochemical characterization studies

The raw materials, the blank and ISO starch dispersions and inks were characterized by means of DSC, XRD, FTIR and TGA analyses (Figure 3). The DSC thermograms of all samples are shown in Figure 3A. Dehydration of both starch dispersions and inks occurred in the temperature range between 60 and 120°C as evidenced by the presence of a broad endothermic peak.[27] ISO exhibited a sharp melting peak at 174°C, the absence of which from the

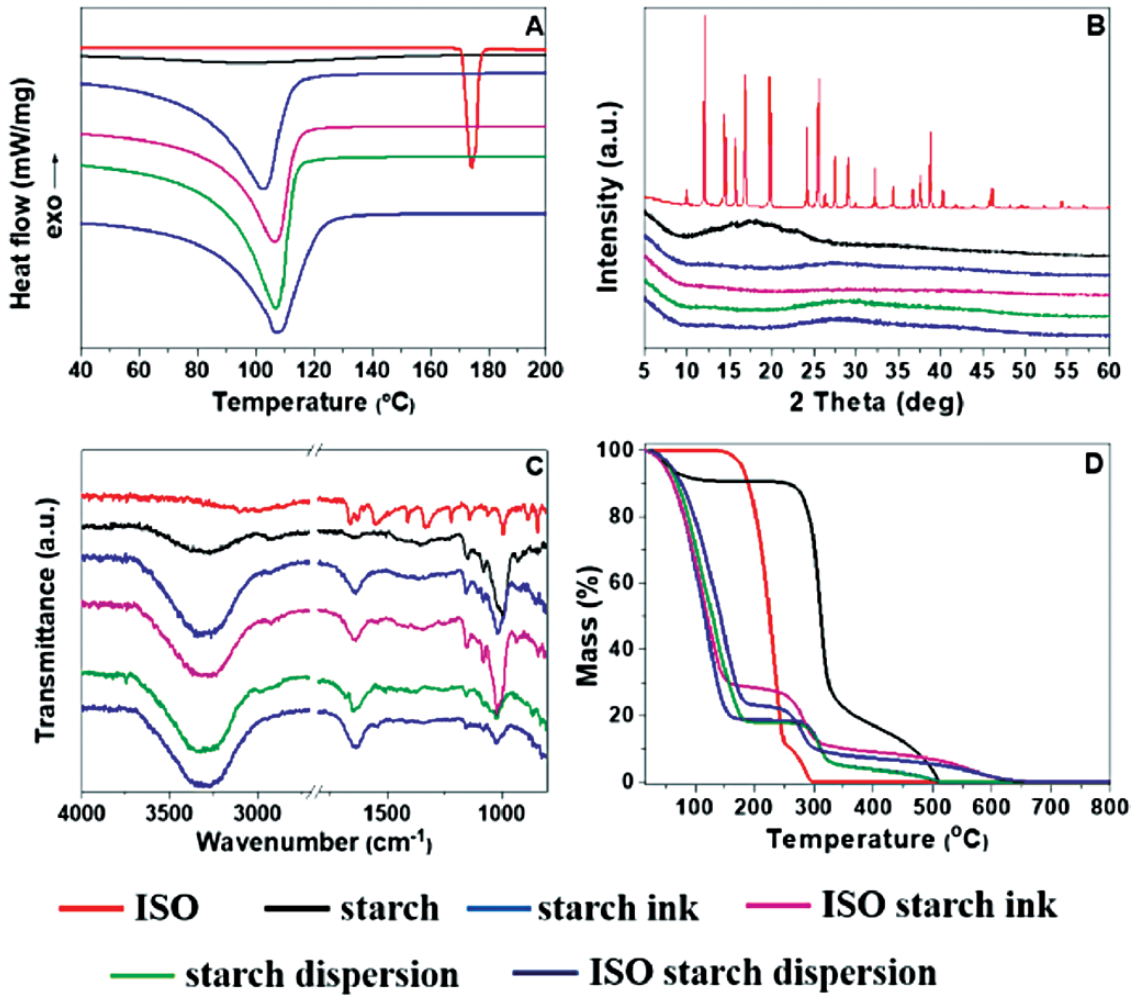

Figure 3 Physicochemical characterization of the raw materials and the blank and ISO starch dispersions and inks by means of (A) DSC, (B) XRD, (C) FTIR and (D) TGA analysis.

thermograms of the ISO starch inks indicates drug amorphization within the hydrogel matrices. The X-ray diffractograms of all samples are illustrated in Figure 3B. Corn starch exhibited a broad amorphous halo at the 2θ range of 10–25°, attributed to its semi-crystalline nature. Starch is a semi-crystalline material consisting of the linear amylose, which contributes to starch's crystallinity and the branched amylopectin, which is responsible for its amorphous phase.[28] Starch amorphization occurred upon dispersion in the water and post gelatinization, owing to the degradation of its ordered phase and the extension of its amorphous phase.[29] None of the diffraction peaks corresponding to crystalline ISO (2θ: 12.1°, 14.3°, 15.6°, 16.8°, 19.7°, 25.5° and 38.7°) were detected in the diffractograms of the ISO starch dispersion and ink, possibly indicating drug amorphization.

FTIR has been used as a tool to investigate starch structure, as well as short-range interactions within its structure.[30] The FTIR spectra of all samples are presented in Figure 3C. Starch spectrum showed peaks at 2930, 1150 and 1000 cm^{-1} attributed to C-H vibration, C-O-H bending and C-O, C-C, C-O-H stretching, respectively.[30] The hydroxyl group present in starch structure is responsible for interaction with water and hydrogel formation. This is why the broad peak observed at 3700–3000 cm^{-1}, which corresponds to the adsorption by excess water, was more pronounced in the starch inks,[30] whereas the presence of an additional peak at 1640 cm^{-1} might originate from the COO^- stretching vibration in the carbohydrate group.[20] Increase in the peak intensity at ca. 1020 cm^{-1} has been associated with more amorphous samples.[31] Starch gelatinization occurs above its glass transition temperature and results in the formation of amorphous starch with molecular disorder,[32] therefore justifying the difference in peak intensity observed between starch inks before and post gelatinization. No characteristic peaks of ISO (C=O stretching: 1664 cm^{-1}, pyridine ring C=N asymmetrical stretching: 1631 cm^{-1} and pyridine ring C=C symmetrical stretching: 1411 cm^{-1}) were detected in the spectra of the ISO starch inks. The TGA curves of all samples are shown in Figure 3D. The thermal decomposition of ISO occurred in two stages between 150–250°C and 250–300°C. Corn starch showed three distinct mass loss stages. The first stage is associated with sample dehydration (25–120°C), followed by a major starch degradation stage (260–350°C) and a third stage, where combustion of residual matter and inorganic components occurs.[33] A similar mass loss pattern was also observed for all starch dispersion and ink samples.

Determination of drug content and dose accuracy

The drug content of the ISO printed tablets was calculated to be 7.95% ± 0.38%, which is in close agreement with the respective value calculated from TGA (8.36%) and corresponds to 97.05% ± 4.68% of the theoretical drug content. Dose accuracy was assessed based on linear regression analysis performed between ISO content in increasing numbers of printed layers. Results indicated a linear correlation (R^2 = 0.9992) between these two variables, suggesting that the intended ISO dose can be precisely adjusted by changing the number of printed layers (Figure 4A).

Water absorption capacity

The water absorption capacity of the blank printed tablets was studied in SGF pH 1.2, and the results are illustrated in Figure 4B. The printed tablets showed a fast water absorption ability within the first 15 min (11.65% ± 2.20%), followed by a more gradual increase up to 75 min, after which equilibrium was attained (17.68% ± 2.24%). The printed tablets retained their structural integrity throughout the study, showing no visible surface degradation.

In-vitro drug release studies

The in-vitro release profile of ISO from the 3D printed soft tablets that had been previously minced to simulate the mastication process was recorded in SGF pH 1.2 at 37°C (Figure 4C). Drug diffusion from the hydrophilic starch-based matrix of the 3D printed soft tablets was rapid with ca. 70% of ISO being released within the first 5 min and almost total drug release achieved within 45 min.

Discussion

This study aims to address the need for paediatric-friendly dosage forms that are developed using safe and cost-effective excipients and enable both ease of administration and dose adjustment based on individual patient needs. To achieve that, we exploited the ability of corn starch, which is a safe and inexpensive excipient, to form extrudable hydrogels upon heat treatment. ISO was used as a model compound owing to the fact that it is recommended in a long-term (of up to 9 months) daily monotherapy course for the treatment of latent tuberculosis infection in children, the efficacy of which is compromised by poor adherence to the current treatment regimen (tablets, syrup and intramuscular injection).[34] SSE 3D printing of starch-based soft dosage forms could, therefore, provide a competitive personalized paediatric-friendly treatment approach for point-of-care and low-resource settings.

The particle size distribution of powder materials used in SSE 3D printing affects their pasting properties, influencing both the precision and resolution of the 3D printed constructs.[35] It is a determinant factor of proper ink printability and may be associated with nozzle-clogging.[36] The use of corn starch with mean particle size of 75 μm indicates the fineness of starch granules used for ink preparation. Thermal treatment induced starch gelatinization, therefore increasing the viscosity of the starch aqueous dispersions,[37] that were then able to be 3D printed in soft dosage forms of varying sizes and child-friendly designs with good printing resolution (Figure 1B and C). This was clearly exemplified after SEM visualization of the freeze-dried 3D printed starch tablets, where a clear distinction of the individual layers deposited one on top of one another was evident. At the same time, a highly porous internal microstructure was observed.

Patient acceptability of a drug dosage form is highly dependent on ease of administration, therefore affecting both treatment adherence and therapeutic outcomes. This is particularly relevant for paediatric patients who may not be able or even be resistant to swallowing solid dosage forms but would be more compliant to an easier to ingest dosage form.[14] This was clearly exemplified in a visual preferences survey of 3D printed tablets conducted in children aged 4–11 years, during which SSE chewable printlets were ranked first on the preference order for the majority of participants.[12] Underpinned by these observations, we aimed at developing a semi-solid dosage form. The starch-based tablets had a soft texture, as identified by the 'two bite test'. All TPA parameters were retained at a minimum, compared with food textures well accepted by children (e.g. fruit or potato puree), which is necessary to facilitate mastication, ease the swallowing process and therefore improve drug intake. At the same time, ease of handling is equally important to ease of swallowing. The starch tablet was easily manipulated after printing, as seen in the inset of Figure 2A

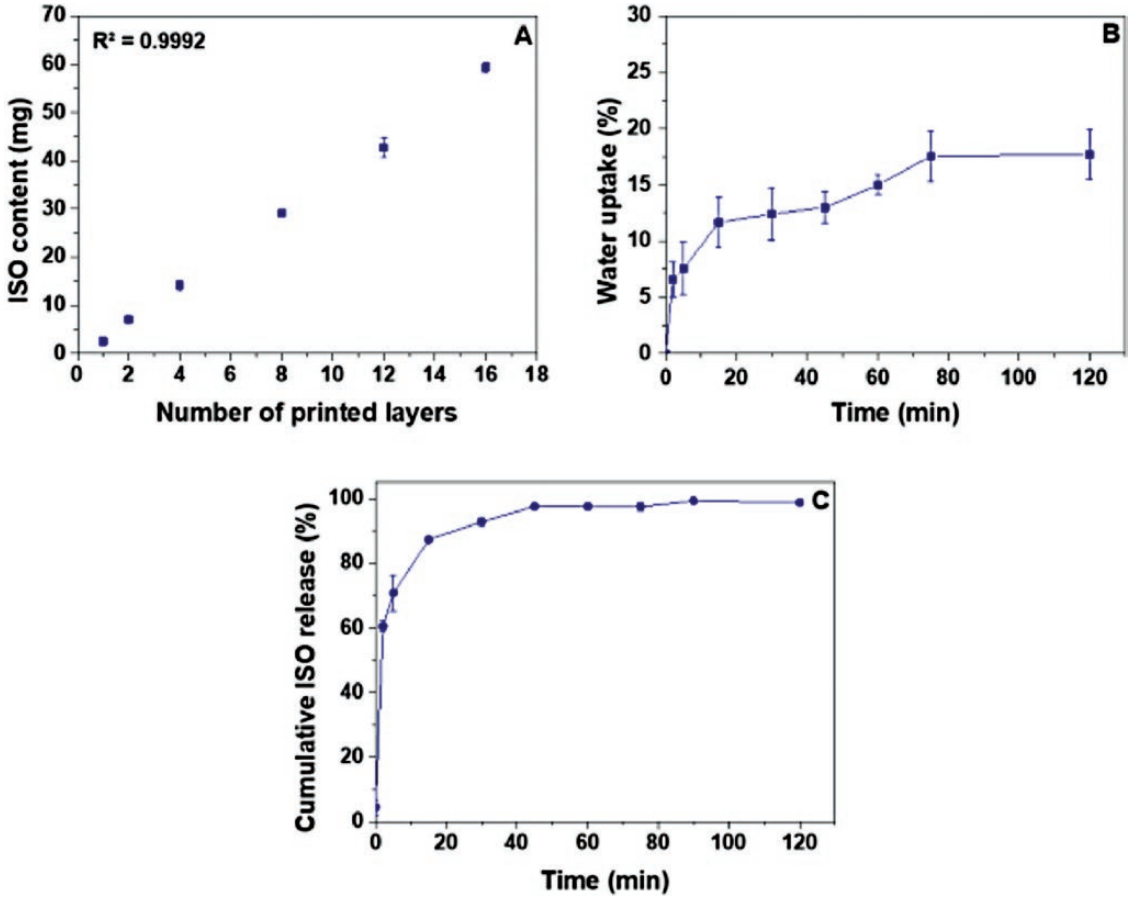

Figure 4 (A) Assessment of dose accuracy with linear regression analysis in the ISO 3D printed starch tablets with increasing number of printed layers ($n = 4 \pm$ S.D.). (B) Water uptake (%) of the 3D printed starch tablets after immersion in SGF for 2 h ($n = 4 \pm$ S.D.). (C) Cumulative ISO release (%) from the 3D printed starch tablets that had been previously minced to simulate the mastication process in SGF at 37°C ($n = 3 \pm$ S.D.).

and further confirmed with rheological studies, which showed the dominancy of the solid-like character of the starch inks (Figure 2B). Physicochemical characterization of the starch inks with DSC and XRD analyses confirmed the presence of ISO in an amorphous state (Figure 3A and B), whereas evidence of starch hydrogelation was provided by FTIR analysis.

Dose accuracy is one of the main requirements for effective and safe pharmacotherapy, especially for paediatric patients for which there is limited availability in a wide spectrum of dosage strengths. Personalization of drug treatment is one of the major assets of 3D printing technologies, enabling precise dose adjustment for each individual patient through changes in the dimensional aspects of a digital design. Within this context, we validated through linear regression analysis that SSE 3D printing of the ISO starch inks enabled dose accuracy in the printed tablets, so that dose could be precisely adjusted to the desired strength by simply changing the number of printed layers.

Starch hydrogels have the ability to absorb water and retain it, resulting in the swelling of their polymer network. Water diffusion occurs into the spaces formed between macromolecule chains and continues until equilibrium state is achieved.[38] Their swelling capacity is attributed to their highly microporous structure that facilitates water penetration within the hydrogel network.[39] Owing to their highly porous microstructure resembling that of a sponge, as already observed with SEM analysis, and high-water absorption and swelling capacity, the starch printed tablets facilitated water penetration within their internal structure, resulting in a ca.17% increase of their initial weight at 2 h after immersion in SGF. This combined with the hydrophilic nature of ISO justifies the fast diffusion of ISO to the release medium, with almost total ISO release attained within 45 min.

Conclusions

The current availability of medicinal products labelled exclusively for use in paediatric patients is limited. The development of age-appropriate dosage forms, using safe and cost-effective excipients, that are both easy to administer and dose titrate is, therefore, essential for effective pharmacotherapy in children. In this study, we aimed to address these requirements from both a material and a manufacturing perspective. We used starch as a safe and cost-effective excipient that could be SSE 3D printed in soft dosage forms, enabling dose titration and accuracy. At the same time, we opted for a material that could be printed in a semi-solid state to overcome the swallowing difficulties commonly encountered with solid dosage forms but could additionally accommodate the use of sweeteners or flavours to potentially enhance palatability. SSE 3D printing of starch-based soft dosage forms could essentially provide a viable paediatric-friendly alternative to manual compounding in hospital settings and an applicable solution in low-resource settings.

Author Contributions

Conceptualization: C.K. and D.G.F.; methodology: C.K., A.-T.C., E.M., N.B. and C.R.; validation: C.K., A.-T.C., E.M., N.B. and C.R.; investigation: C.K., A.-T.C. and E.M.; resources: D.G.F.; writing—original draft preparation: C.K., A.-T.C., E.M., N.B. and C.R.; writing—review and editing: C.K. and D.G.F.; supervision: C.K. and D.G.F.; funding acquisition: D.G.F.

Funding

This research received no specific grant from any funding agency in the public, commercial, or not-for-profit sectors.

Conflicts of Interest

The authors declare no conflicts of interest.

References

1. Gioumouxouzis CI, Karavasili C, Fatouros DG. Recent advances in pharmaceutical dosage forms and devices using additive manufacturing technologies. *Drug Discov Today* 2019; 24: 636–43. http://doi.org/10.1016/j.drudis.2018.11.019
2. Firth J, Basit AW, Gaisford S. The role of semi-solid extrusion printing in clinical practice. In: Basit AW, Gaisford S (eds.), *3D Printing of Pharmaceuticals*. Cham: Springer International Publishing, 2018, 133–151.
3. Seoane-Viaño I, Januskaite P, Alvarez-Lorenzo C *et al*. Semi-solid extrusion 3D printing in drug delivery and biomedicine: personalised solutions for healthcare challenges. *J Control Release* 2021; 332: 367–89. http://doi.org/10.1016/j.jconrel.2021.02.027
4. Rahman J, Quodbach J. Versatility on demand—the case for semi-solid micro-extrusion in pharmaceutics. *Adv Drug Deliv Rev* 2021; 172: 104–26. http://doi.org/10.1016/j.addr.2021.02.013
5. Khaled SA, Burley JC, Alexander MR *et al*. 3D printing of five-in-one dose combination polypill with defined immediate and sustained release profiles. *J Control Release* 2015; 217: 308–14. http://doi.org/10.1016/j.jconrel.2015.09.028
6. Khaled SA, Burley JC, Alexander MR *et al*. 3D printing of tablets containing multiple drugs with defined release profiles. *Int J Pharm* 2015; 494: 643–50. http://doi.org/10.1016/j.ijpharm.2015.07.067
7. El Aita I, Breitkreutz J, Quodbach J. On-demand manufacturing of immediate release levetiracetam tablets using pressure-assisted microsyringe printing. *Eur J Pharm Biopharm* 2019; 134: 29–36. http://doi.org/10.1016/j.ejpb.2018.11.008
8. Khaled SA, Alexander MR, Wildman RD *et al*. 3D extrusion printing of high drug loading immediate release paracetamol tablets. *Int J Pharm* 2018; 538: 223–30. http://doi.org/10.1016/j.ijpharm.2018.01.024
9. El Aita I, Rahman J, Breitkreutz J *et al*. 3D-printing with precise layer-wise dose adjustments for paediatric use via pressure-assisted microsyringe printing. *Eur J Pharm Biopharm* 2020; 157: 59–65. http://doi.org/10.1016/j.ejpb.2020.09.012
10. Goyanes A, Madla CM, Umerji A *et al*. Automated therapy preparation of isoleucine formulations using 3D printing for the treatment of MSUD: first single-centre, prospective, crossover study in patients. *Int J Pharm* 2019; 567: 118497. http://doi.org/10.1016/j.ijpharm.2019.118497
11. Karavasili C, Gkaragkounis A, Fatouros DG. Patent landscape of pediatric-friendly oral dosage forms and administration devices. *Expert Opin Ther Pat* 2021; 31: 663–86. http://doi.org/10.1080/13543776.2021.1893691
12. Januskaite P, Xu X, Ranmal SR *et al*. I spy with my little eye: a paediatric visual preferences survey of 3D printed tablets. *Pharmaceutics* 2020; 12: 1100. http://doi.org/10.3390/pharmaceutics12111100
13. Karavasili C, Gkaragkounis A, Moschakis T *et al*. Pediatric-friendly chocolate-based dosage forms for the oral administration of both hydrophilic and lipophilic drugs fabricated with extrusion-based 3D printing. *Eur J Pharm Sci* 2020; 147: 105291. http://doi.org/10.1016/j.ejps.2020.105291
14. Nunn T, Williams J. Formulation of medicines for children. *Br J Clin Pharmacol* 2005; 59: 674–6. http://doi.org/10.1111/j.1365-2125.2005.02410.x
15. Öblom H, Zhang J, Pimparade M *et al*. 3D-printed isoniazid tablets for the treatment and prevention of tuberculosis—personalized dosing and drug release. *AAPS PharmSciTech* 2019; 20: 52. http://doi.org/10.1208/s12249-018-1233-7
16. Ghanizadeh Tabriz A, Nandi U, Hurt AP *et al*. 3D printed bilayer tablet with dual controlled drug release for tuberculosis treatment. *Int J Pharm* 2021; 593: 120147. http://doi.org/10.1016/j.ijpharm.2020.120147
17. Genina N, Boetker JP, Colombo S *et al*. Anti-tuberculosis drug combination for controlled oral delivery using 3D printed compartmental dosage forms: from drug product design to *in vivo* testing. *J Control Release* 2017; 268: 40–8. http://doi.org/10.1016/j.jconrel.2017.10.003
18. Mateescu MA, Ispas-Szabo P, Assaad E. (eds.). Chapter 2—Starch and derivatives as pharmaceutical excipients: from nature to pharmacy. In: *Woodhead Publishing Series in Biomedicine*. Cambridge: Woodhead Publishing, 2015, 21–84.
19. Spyridis NP, Spyridis PG, Gelesme A *et al*. The effectiveness of a 9-month regimen of isoniazid alone versus 3- and 4-month regimens of isoniazid plus rifampin for treatment of latent tuberculosis infection in children: results of an 11-year randomized study. *Clin Infect Dis* 2007; 45: 715–22. http://doi.org/10.1086/520983
20. Zheng L, Yu Y, Tong Z *et al*. The characteristics of starch gels molded by 3D printing. *J Food Process Preserv* 2019; 43: e13993. http://doi.org/10.1111/jfpp.13993
21. Yang F, Zhang M, Bhandar B *et al*. Investigation on lemon juice gel as food material for 3D printing and optimization of printing parameters. *LWT—Food Sci Technol* 2018; 87: 67–76. http://doi.org/10.1016/j.lwt.2017.08.054
22. Hedayati S, Niakousari M. Microstructure, pasting and textural properties of wheat starch-corn starch citrate composites. *Food Hydrocoll* 2018; 81: 1–5. http://doi.org/10.1016/j.foodhyd.2018.02.024
23. Park JW, Lee S, Yoo B *et al*. Effects of texture properties of semi-solid food on the sensory test for pharyngeal swallowing effort in the older adults. *BMC Geriatr* 2020; 20: 493. http://doi.org/10.1186/s12877-020-01890-4
24. Hwang J, Kim DK, Bae JH *et al*. The effect of rheological properties of foods on bolus characteristics after mastication. *Ann Rehabil Med* 2012; 36: 776–84. http://doi.org/10.5535/arm.2012.36.6.776
25. Miller KA, Hoseney RC. Dynamic rheological properties of wheat starch-gluten doughs. *Cereal Chem* 1999; 76: 105–9. http://doi.org/10.1094/CCHEM.1999.76.1.105
26. Alias SA, Mhd Sarbon N. Rheological, physical, and mechanical properties of chicken skin gelatin films incorporated with potato starch. *NPJ Sci Food* 2019; 3: 26. http://doi.org/10.1038/s41538-019-0059-3
27. Dehabadi L, Karoyo AH, Wilson LD. Spectroscopic and thermodynamic study of biopolymer adsorption phenomena in heterogeneous solid-liquid systems. *ACS Omega* 2018; 3: 15370–9. http://doi.org/10.1021/acsomega.8b01663
28. Liu H, Yu L, Xie F *et al*. Gelatinization of cornstarch with different amylose/amylopectin content. *Carbohydr Polym* 2006; 65: 357–63. http://doi.org/10.1016/j.carbpol.2006.01.026
29. Liu H, Xie F, Yu L *et al*. Thermal processing of starch-based polymers. *Prog Polym Sci* 2009; 34: 1348–68. http://doi.org/10.1016/j.progpolymsci.2009.07.001
30. Warren FJ, Gidley MJ, Flanagan BM. Infrared spectroscopy as a tool to characterise starch ordered structure—a joint FTIR-ATR, NMR, XRD and DSC study. *Carbohydr Polym* 2016; 139: 35–42. http://doi.org/10.1016/j.carbpol.2015.11.066
31. Capron I, Robert P, Colonna P *et al*. Starch in rubbery and glassy states by FTIR spectroscopy. *Carbohydr Polym* 2007; 68: 249–59. http://doi.org/10.1016/j.carbpol.2006.12.015

32. Jouppila K, Roos YH. The physical state of amorphous corn starch and its impact on crystallization. *Carbohydr Polym* 1997; 32: 95–104. http://doi.org/10.1016/S0144-8617(96)00175-0
33. LeCorre D, Bras J, Dufresne A. Influence of native starch's properties on starch nanocrystals thermal properties. *Carbohydr Polym* 2012; 87: 658–66. http://doi.org/10.1016/j.carbpol.2011.08.042
34. Assefa Y, Assefa Y, Woldeyohannes S *et al.* 3-Month daily rifampicin and isoniazid compared to 6- or 9-month isoniazid for treating latent tuberculosis infection in children and adolescents less than 15 years of age: an updated systematic review. *Eur Respir J* 2018; 52: 1800395. http://doi.org/10.1183/13993003.00395-2018
35. Godoi FC, Prakash S, Bhandari BR. 3D printing technologies applied for food design: status and prospects. *J Food Eng* 2016; 179: 44–54. http://doi.org/10.1016/j.jfoodeng.2016.01.025
36. Theagarajan R, Moses JA, Anandharamakrishnan C. 3D extrusion printability of rice starch and optimization of process variables. *Food Bioprocess Technol* 2020; 13: 1048–62. http://doi.org/10.1007/s11947-020-02453-6
37. Höfer R. Chapter 4A—Sugar- and starch-based biorefineries. In: Pandey A, Höfer R, Taherzadeh M *et al.* (eds.), *Industrial Biorefineries and White Biotechnology*. Amsterdam: Elsevier, 2015: 157–235.
38. Witono JR, Noordergraaf IW, Heeres HJ *et al.* Water absorption, retention and the swelling characteristics of cassava starch grafted with polyacrylic acid. *Carbohydr Polym* 2014; 103: 325–32. http://doi.org/10.1016/j.carbpol.2013.12.056
39. Biduski B, Silva WMFD, Colussi R *et al.* Starch hydrogels: the influence of the amylose content and gelatinization method. *Int J Biol Macromol* 2018; 113: 443–9. http://doi.org/10.1016/j.ijbiomac.2018.02.144